JOURNAL OF THE ROYAL SOCIETY Interface

rsif.royalsocietypublishing.org

Research

Cite this article: Pongrac P, Kreft I, Vogel-Mikuš K, Regvar M, Germ M, Vavpetič P, Grlj N, Jeromel L, Eichert D, Budič B, Pelicon P. 2013 Relevance for food sciences of quantitative spatially resolved element profile investigations in wheat (*Triticum aestivum*) grain. J R Soc Interface 10: 20130296.
http://dx.doi.org/10.1098/rsif.2013.0296

Received: 2 April 2013
Accepted: 25 April 2013

Subject Areas:
biophysics

Keywords:
wheat, zinc, cadmium, iron, lead, localization analysis

Author for correspondence:
Ivan Kreft
e-mail: ivan.kreft@guest.arnes.si

Electronic supplementary material is available at http://dx.doi.org/10.1098/rsif.2013.0296 or via http://rsif.royalsocietypublishing.org.

Royal Society Publishing
Informing the science of the future

Relevance for food sciences of quantitative spatially resolved element profile investigations in wheat (*Triticum aestivum*) grain

Paula Pongrac[1], Ivan Kreft[1], Katarina Vogel-Mikuš[1], Marjana Regvar[1], Mateja Germ[1], Primož Vavpetič[2], Nataša Grlj[2], Luka Jeromel[2], Diane Eichert[3], Bojan Budič[4] and Primož Pelicon[2]

[1]Biotechnical Faculty, University of Ljubljana, Jamnikarjeva 101, 1000 Ljubljana, Slovenia
[2]Jožef Stefan Institute, Jamova 39, 1000 Ljubljana, Slovenia
[3]Sincrotrone Trieste, Area Science Park, S.S. 14, km 163.5, 34149 Trieste, Italy
[4]National Institute of Chemistry, Hajdrihova 19, 1000 Ljubljana, Slovenia

Bulk element concentrations of whole grain and element spatial distributions at the tissue level were investigated in wheat (*Triticum aestivum*) grain grown in Zn-enriched soil. Inductively coupled plasma mass spectrometry and inductively coupled plasma optical emission spectrometry were used for bulk analysis, whereas micro-proton-induced X-ray emission was used to resolve the two-dimensional localization of the elements. Soil Zn application did not significantly affect the grain yield, but did significantly increase the grain Ca, Fe and Zn concentrations, and decrease the grain Na, P and Mo concentrations; bulk Mg, S, K, Mn, Cu, Cd and Pb concentrations remained unchanged. These changes observed in bulk element concentrations are the reflection of tissue-specific variations within the grain, revealing that Zn application to soil can lead to considerable alterations in the element distributions within the grain, which might ultimately influence the quality of the milling fractions. Spatially resolved investigations into the partitioning of the element concentrations identified the tissues with the highest element concentrations, which is of utmost importance for accurate prediction of element losses during the grain milling and polishing processes.

1. Introduction

Significant progress has been achieved in the worldwide fight against Zn and Fe malnutrition, which are considered as the two elements that are the most severely lacking in diets [1]. In this framework, assessing and improving the nutritional quality of cereal crops is of major importance [2], and especially in the case of wheat (*Triticum aestivum* L.), which is one of the most consumed cereals. Fertilization of plants (i.e. agronomic biofortification), for instance to provide a large pool of Zn in vegetative tissues during grain filling, constitutes a sound alternative to increasing the element contents in cereals [3]. Transgenic approaches to increase the element contents of cereal grains have also been considered, such as manipulation of the transporters involved in the uptake and translocation of various elements [4]. In general, technologically induced increases in Zn grain concentrations through Zn fertilization are expected to have positive effects on human health in areas of Zn malnutrition [1].

In metal-enriched soils, relatively high amounts of undesirable elements can accumulate in plant tissues without any visible symptoms of toxicity, and can subsequently be transferred through the food chain, where they can be biomagnified [1]. For example, intensive agriculture production systems that make use of phosphate fertilizers, or anthropogenically related pollution are the main sources of Cd contamination in soils. Such elevated Cd concentrations constitute a public health threat, as Cd concentrations in grain depend primarily

on the amount of Cd that is bioavailable to plants [5], which can consequently lead to potential accumulation of Cd in grains. Furthermore, the soil environmental factors, such as pH, organic matter content, and presence of other ions in the soil solution, have a great influence on Cd availability, through ionic strength effects, complexation processes and competition for soil– and root–surface exchange sites [6]. In this framework, to take advantage of the differential affinities of the ion transporters for Zn and Cd uptake [7], the application of Zn fertilizers has been proposed to reduce Cd concentrations in the grain. In durum wheat (*Triticum durum*), for example, Cd application can affect Zn concentrations in shoots, depending on the Zn nutrient status of the plant [8].

Determining the total concentrations of elements in grain by bulk element analysis is, however, not an effective way to predict the nutritive value of the grains under investigation. Elements such as P, K, Ca, Mn, Fe and Zn are, indeed, unevenly distributed across the different grain tissues, with a preferential accumulation in the aleurone layer, embryo and testa, from where they are frequently lost during grain processing [9–11]. Micro-beam techniques are therefore essential characterization tools to assess the spatial localization of the elements at the tissue level, and to reveal their potential co-localization. Among them, micro-proton-induced X-ray emission (micro-PIXE) is a fully quantitative technique that can simultaneously detect the elements from Na to U with a spatial resolution of 1 μm. This multi-element analysis has already been successfully applied in various studies of essential elements and contaminants in different plant and animal tissues [12–15].

The main aim of this study was to determine the element profiles within the different tissues of wheat grain, to define any alterations in the relative partitioning of the mineral elements that might take place during Zn fertilization of wheat plants. This repartitioning will ultimately influence the quality of the milling fractions of the grain. Element concentration profiles enable, in particular, identification of the specific tissue with the highest element concentrations, which is a prerequisite for predicting mineral losses during grain polishing and for the allocation of elements among the milling fractions.

2. Material and methods

2.1. Plant material and sample preparation

Wheat (*T. aestivum* cv. Reska) was grown in Mitscherlich containers (20×21.5 cm diameter × height, respectively; containing 7 kg soil per container) at the experimental field of the Biotechnical Faculty, University of Ljubljana, Ljubljana, Slovenia (320 m.a.s.l.; 46°35′ N, 14°55′ E). The soil used was collected from an inhabited area in northern Slovenia (Žerjav) that has numerous vegetable gardens, and which is also a locality that is well known for its high soil Cd, Zn and Pb concentrations. The following soil properties were determined: pseudo-total soil concentrations of 30.4 ± 0.3 mg Cd kg^{-1} soil, 1826 ± 61 mg Zn kg^{-1} soil and 4603 ± 94 mg Pb kg^{-1} soil; pH 6.6–7.0; organic matter, 11.3% ± 0.4%; total N, 0.48% ± 0.01%; carbonate, 20.2% ± 1.5%; sand, 42% ± 1%; silt, 47.5% ± 1.4%; clay, 10.5% ± 0.4%; P_2O_5, 133 ± 1.8 mg $100\ g^{-1}$ soil; and K_2O, 28.2 ± 1.8 mg $100\ g^{-1}$ soil [16]. The exchangeable fractions of Cd, Zn and Pb were 7.6% ± 0.1%, 2.0% ± 0% and 0.3% ± 0%, respectively [16]. Each of the two containers in each treatment group contained from 15 to 25 plants. To increase the concentrations of Zn in the soil, 1.0 g Zn kg^{-1} soil (in nitrate form) was added to the soil. After 95 days of growth, the mature grain was collected for each treatment group from five randomly chosen plants from each container. The grain was air dried, and the dry weight (DW) of the whole grain for each plant (grain yield) was determined (g). The grain was stored in paper bags until the analyses.

2.2. Bulk element concentration, content and statistical analyses

For bulk element concentration analysis, four subsamples (each of approx. 1 g) from a composite sample of all of the grain from each treatment were homogenized in liquid nitrogen using a pestle and mortar. About 0.1 g of this powdered material was digested in 3 ml HNO_3 and 0.5 ml H_2O_2 in quartz vessels, using the Milestone microwave sample digestion system (Ethos 1). After thermal treatment of three 10 min steps at different temperatures (130°C, 180°C, 18°C), the cooled digests were transferred to 25 ml beakers, diluted to 25 ml with Milli-Q water and kept in a refrigerator until analysis.

All of the digestions were diluted 10-fold in Milli-Q water before the measurements. The K, Na, P, Ca and S concentrations were determined using inductively coupled plasma optical emission spectroscopy (ICP-OES; Varian 715 ES radially view), and Mg, Mn, Fe, Cu, Zn, Mo, Cd and Pb concentrations were determined using inductively coupled plasma mass spectrometry (ICP-MS; Agilent 7500 ce, equipped with a collision/reaction cell), according to the manufacturer recommendations. For both techniques, multi-element calibration solutions were prepared from a 1 mg ml^{-1} single stock standard solution (Merck, Darmstadt, Germany). The analyte concentrations for the ICP-OES calibration ranged from 0 to 10 mg l^{-1}, and for the ICP-MS from 0 to 1 mg l^{-1}.

Total element content (μg per plant) was calculated by multiplying bulk element concentration with grain yield.

Differences in element concentrations and contents between the two treatments were tested using Student's *t*-test (StatSoft Statistica, v. 8.0), and differences were considered significant at $p < 0.05$.

2.3. Element mapping and profiling by micro-proton-induced X-ray emission

For the analyses at the tissue level, the grain was sliced twice with a sharp stainless steel razor, perpendicular to the grain length, to obtain a thick cross section that had two flat edges. Additionally, mature wheat grain was soaked overnight in Milli-Q water and cut in half with a sharp stainless steel razor. These halves were quickly transferred into Al foil beds ($0.5 \times 0.5 \times 0.5$ cm) that contained a drop of distilled water, and rapidly frozen in liquid nitrogen. The frozen samples were transferred to a cryo-microtome (Leica CM3050) chamber where they were glued onto a sample holder with tissue-freezing medium (Jung, Leica Microsystems, Nussloch, Germany), to ensure the stability of the sample. Cryosectioning of 60 μm (thin) sections was performed at −25°C, using disposable stainless steel cryo-microtome blades. The sections were examined using the dissecting binocular attached to the cryo-microtome, and placed on pre-cooled filter paper in custom-designed pre-cooled Al beakers with a fitting stainless steel cover. The specimens were transferred to a freeze dryer (Alpha 2-4 Christ; Gefriertrocknungsanlagen GmbH, Osterode am Harz, Germany) in liquid nitrogen, and freeze-dried at −30°C and 0.34 mbar for 2 days. The thick and thin cross sections were mounted between two thin layers of Pioloform foil [17] (SPI Supplies, West Chester, PA, USA), stretched on an Al holder, and

Table 1. Bulk concentrations, contents and the section-specific concentrations of the elements in whole grain of wheat grown in non-fertilized and Zn-fertilized soil. Data are means ± standard errors. Bulk concentrations were measured with ICP-MS and ICP-OES; $n = 4$. Total element content was calculated by multiplying bulk element concentration with grain yield. Section-specific concentrations were calculated from numerical matrices generated by GeoPIXEII software from micro-PIXE scans at each grain cross section using the ImageJ program [22]; $n = 3$. LOD, below the limit of detection.

	bulk concentrations (mg kg^{-1})		content (μg plant^{-1})		section-specific concentrations (mg kg^{-1})	
	non-fertilized	Zn-fertilized	non-fertilized	Zn-fertilized	non-fertilized	Zn-fertilized
Na	34.3 ± 1.52	28.2 ± 1.09[a]	119 ± 5.27	83.4 ± 3.23[a]	LOD	LOD
Mg	2460 ± 138	2340 ± 82.7	8570 ± 479	6920 ± 244[a]	2560 ± 155	2630 ± 1370
P	7210 ± 265	6290 ± 228[a]	25 100 ± 921	18 600 ± 675[a]	7410 ± 2180	6480 ± 1470
S	2270 ± 17.7	2310 ± 47.8	7910 ± 61.5	6830 ± 141	1220 ± 495	1650 ± 657
K	6110 ± 325	5560 ± 254	21 270 ± 1130	16 400 ± 751[a]	7390 ± 1210	5380 ± 845
Ca	323 ± 12.8	461 ± 22.2[a]	1120 ± 44.4	1360 ± 65.6[a]	502 ± 33.8	695 ± 43.9
Mn	10.3 ± 0.38	9.89 ± 0.74	35.7 ± 1.31	29.2 ± 2.19[a]	23.2 ± 7.46	13.6 ± 0.76
Fe	68.8 ± 3.60	118 ± 16.7[a]	240 ± 12.5	349 ± 49.4[a]	87.7 ± 14.0	130 ± 13.4
Cu	10.3 ± 0.40	9.65 ± 0.78	35.8 ± 1.38	28.5 ± 2.29[a]	17.7 ± 3.70	13.8 ± 0.92
Mo	8.20 ± 0.28	6.32 ± 0.13[a]	28.5 ± 0.97	18.7 ± 0.39[a]	LOD	LOD
Zn	89.5 ± 5.49	220 ± 25.1[a]	311 ± 19.10	651 ± 74.2[a]	141 ± 30.9	241 ± 10.9
Cd	1.06 ± 0.28	0.83 ± 0.06	3.67 ± 0.96	2.45 ± 0.17[a]	LOD	LOD
Pb	0.33 ± 0.03	0.45 ± 0.05	1.16 ± 0.10	1.33 ± 0.13	LOD	LOD

[a]Statistically significant differences between non-fertilized and Zn-fertilized plants (Student's t-test, $p < 0.05$).

kept in a desiccator together with silica gel until analysis. Three samples per treatment were measured with micro-PIXE to ensure the relevance of the data.

Micro-PIXE analysis was performed using the nuclear microprobe at the Jožef Stefan Institute [18,19]. A 3 MeV proton beam was used, with ion current ranging from 100 to 500 pA, and a beam diameter varying from 1 to 3 μm. The detection of the outcoming X-rays, from 1 up to 25 keV in energy, was ensured by a pair of X-ray detectors: a high-purity Ge X-ray detector (95 mm^2 active area, 25 μm thick Be window, 100 μm thick polyimide absorber) positioned at an angle of 135° with respect to the beam direction; and a Si(Li) detector (10 mm^2 area, 8 μm thick Be window, for detecting the lower X-ray energies from 0.8 to 4 keV) positioned at an angle of 125° with respect to the beam direction. The samples were sprayed with low-energy electrons obtained from a hot tungsten filament during the measurements to avoid sample charging, thus efficiently avoiding time-consuming specimen carbon coating. The proton dose was determined with an in-beam chopping device (gold-plated graphite) positioned in the X-ray beam path just prior to the sample. The rotating chopper periodically intersected the beam, at a frequency of approximately 10 Hz, which made the proton dose measurements insensitive to beam intensity fluctuations. The spectrum of backscattered protons from the chopper was recorded together with the micro-PIXE spectra. The high-energy part of the spectrum consists of protons scattered from the Au layer, appearing as a separate peak, the area of which is proportional to the proton flux. During offline data processing, the proton dose that corresponds to an arbitrary area selection within the scanning frame can be extracted offline from the list-mode results, simultaneous with the micro-PIXE spectra [20]. The calibration of the micro-PIXE measurements was verified by analysis of multi-element standard reference materials: NIST SRM 1573a (tomato leaves, homogenized powder, analysed in the form of a pressed pellet); NIST SRM 1107 (naval brass B, alloy); and NIST SRM 620 (soda-lime flat glass).

The micro-PIXE data were analysed using the GeoPIXEII software package [21], which generated quantitative element distribution maps and element distribution profiles for the chosen transects. The corresponding concentrations of the elements (referred to as the section-specific concentrations) were extracted from the numerical matrices of each element distribution map and for each grain cross section obtained with GeoPIXEII software, and processed with ImageJ [22].

The micrographic images of the thick cross sections of the whole grain were obtained with a Stemi SV 11 stereomicroscope (Carl Zeiss; Goettingen, Germany), whereas 60 μm cross sections were examined with an Axioskop 2 MOT microscope (Carl Zeiss), using a UV-light excitation source. The images were obtained with an Axiocam MRc colour digital camera, using AxioVision v. 4.1 software.

3. Results

3.1. Grain yield, bulk element concentrations and contents

Despite high Cd, Zn and Pb concentrations in the soil, the wheat plants showed no visible toxicity symptoms (not shown). The grain yield (whole DW of grain per plant) was highly variable and it did not differ significantly between the non-fertilized plants (mean 3.48 ± 1.29 g) and the Zn-fertilized plants (mean 2.96 ± 1.14 g). Nevertheless, Zn fertilization led to significant increases in bulk Ca, Fe and Zn concentrations and decreased bulk Na, P and Mo concentrations; bulk Mg, S, K, Mn and Cu concentrations remained unchanged (table 1). The changes in the concentrations of toxic Cd and Pb owing to this Zn fertilization were not statistically significant. However, when expressed

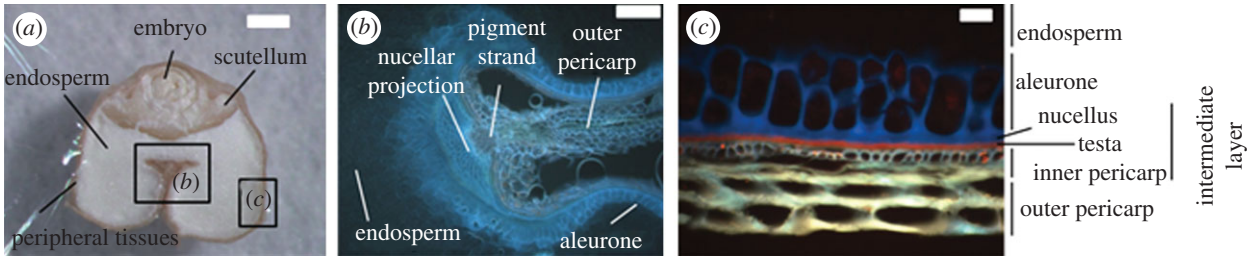

Figure 1. Morphological structures of cross-sectioned wheat grain as seen under the stereomicroscope (*a*) thick section (scale bar, 500 μm) and under the microscope using a UV-light excitation source (*b*) thin section (scale bar, 200 μm); (*c*) thin section (scale bar, 20 μm).

as the total contents (element concentration multiplied by grain yield), the changes in Na, Mg, P, K, Ca, Mn, Fe, Cu, Mo, Zn and Cd owing to Zn fertilization were significant (table 1). The raw data of the bulk element concentrations, grain yields and whole grain element contents are given in the electronic supplementary material, tables S1, S2 and S3, respectively.

3.2. Spatially resolved element distributions in grain tissues

Element localization within particular tissues of the wheat grain was assessed by micro-PIXE analysis. The area selected (2000 × 2000 μm) included all of the relevant and easily identifiable tissues in the grain (figure 1*a*). The quantitative element maps generated (figure 2) primarily uncovered the specific distributions of the elements within the different grain tissues. To simplify the quantitative visualization of the distribution of these element concentrations within the particular tissues, element-concentration profiles across chosen transects (traversing the majority of the tissues of the grain) were built; these are referred to as the element distribution profiles (figure 2). Owing to the tissue size variability between the differing specimens, the concentration peaks of the elements in particular tissues were overlaid manually. This visualization allows easy and direct comparison of the element concentrations in the two specimens analysed, and thus within the tissues identified: crease aleurone, pigment strand, nucellar projection, aleurone, endosperm, scutellum, embryo and peripheral layers (as indicated in figure 1*b*,*c*). Unfortunately, the concentrations of Cd and Pb were below the detection limits of micro-PIXE, as were also the concentrations of Na and Mo, whereas other section-specific concentrations of Mg, P, S, K, Ca, Mn, Fe, Cu and Zn were determined with ImageJ from the numerical matrices generated by GeoPIXEII software from micro-PIXE scans at each grain cross section (table 1; see also electronic supplementary material, table S4 for the raw data of the concentrations for each cross section).

The direct comparison of the element distribution profiles in the grain of non-fertilized and Zn-fertilized wheat plants revealed localized changes in the element concentrations in specific grain tissues (figure 2). After Zn application to the soil, the concentrations of P, K, Fe and Zn were higher in the crease aleurone layer, scutellum and embryo, whereas the Ca concentrations were higher in the pigment strand and nucellar projection. These variations in concentrations can also be observed in the element maps, with additional information on the distributions of the selected elements within the particular grain tissues. In the grain of non-fertilized plants, however, there were higher concentrations of S and Cu in the nucellar projection, and of Mn in the pigment strand. Nevertheless, owing to the smaller portions of both these tissues, their contributions to the overall grain concentrations were negligible.

As the local heterogeneity of the element distributions is of primary importance, such as in the peripheral aleurone layer where nutrients and minerals are preferentially stored, thin sections (60 μm) were also analysed with micro-PIXE. The element maps (300 × 300 μm) revealed the predominant local accumulation of P, K, Fe, Cu and Zn inside the aleurone cells, of S in specific subaleurone endosperm cells, and of Ca and Mn in the intermediate layer (composed of nucellus, testa and inner pericarp tissues), with Ca deposition also in the outer pericarp and in distinct 'hotspots' within the endosperm (figure 3).

4. Discussion

The concentrations of Cd, Zn and Pb in metal-enriched soil from Žerjav (Slovenia) used in this study exceed the legal thresholds of maximum tolerable concentrations (12, 720 and 530 mg kg^{-1}, respectively). Thus, according to Slovenian legislation [23], this soil is not appropriate for growing crops. Despite this, crops and vegetables are grown in this heavily metal-polluted area, and are used for human and animal consumption, with more or less acute consequences for health [24]. Crops differ markedly in their uptake of metals and their susceptibility to metal toxicity. No visible toxicity symptoms were observed for the plants in this study, and the plants completed their life cycle and formed grain in this soil despite the high Cd and Pb concentrations. This indicates that the Reska wheat variety, which has also been demonstrated to be a heat-tolerant wheat genotype [25], might also be metal tolerant. Nevertheless, the bulk grain concentrations in both the non-fertilized and the Zn-fertilized wheat exceeded the upper tolerable intake levels for Cd and Pb (0.2 mg kg^{-1} [26]) by up to fourfold, making these grains unsuitable for human consumption.

A fourfold higher bulk Zn concentration (89.5 ± 5.49 mg kg^{-1}) and a 1.8-fold higher bulk Fe concentration (68.8 ± 3.60 mg kg^{-1}) were measured in the grain of the non-fertilized wheat plants, compared with typical average Zn and Fe concentrations of 21.4 and 38.2 mg kg^{-1}, respectively, that have been reported for bread wheat grain [27]. This suggests that this Reska wheat, which was bred for high protein content, has efficient Zn and Fe acquisition, transport and/or phloem-unloading mechanisms. These mechanisms are a prerequisite for high grain Zn and Fe concentrations despite initial high Zn concentration in the non-fertilized soil. The pronounced increases in grain element concentrations as well as in grain element contents observed indicate that the fertilization with Zn nitrate had significant

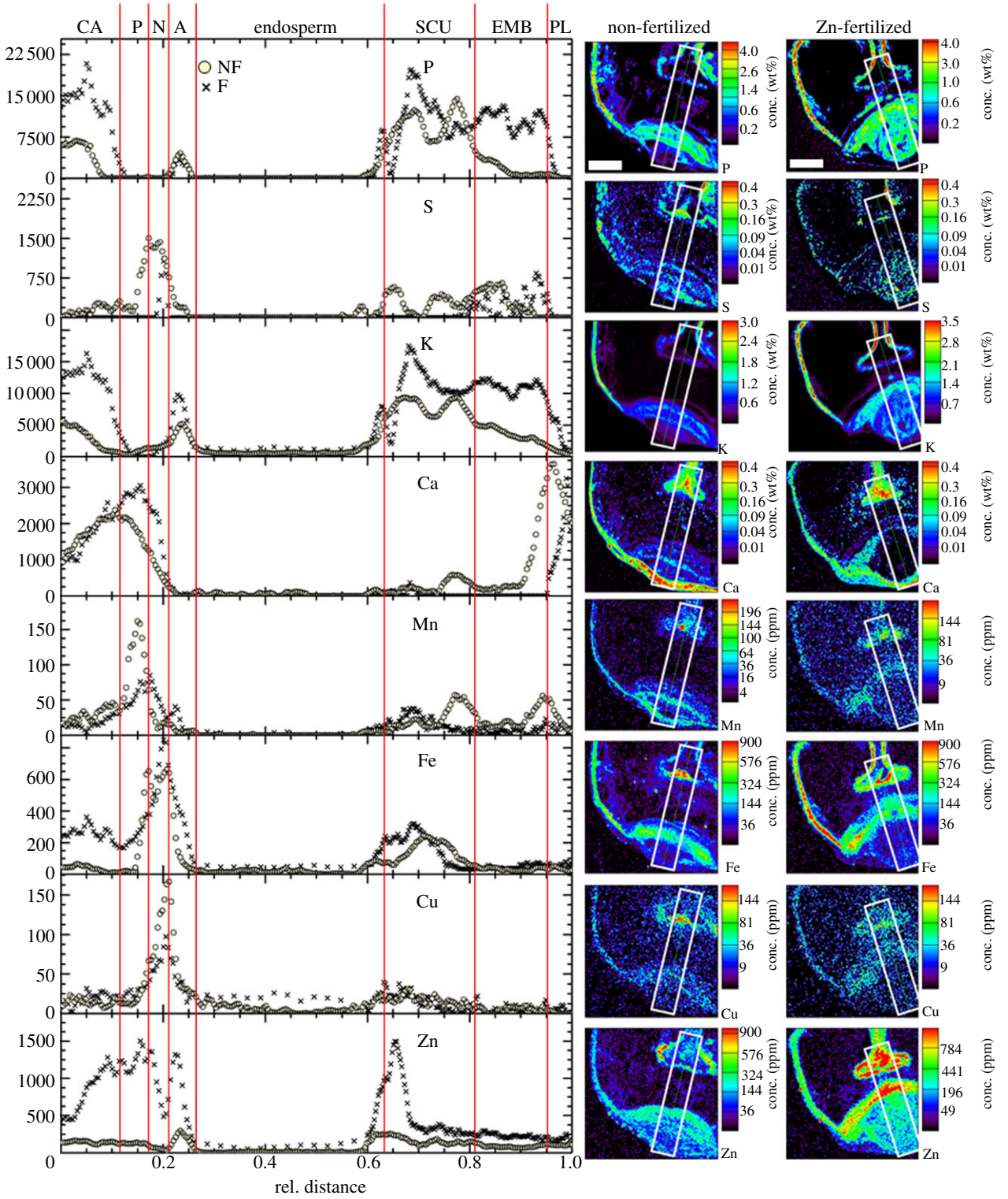

Figure 2. Element distribution profiles and micro-PIXE quantitative element maps from grain cross sections of wheat grown in non-fertilized (circles) and Zn-fertilized (crosses) soils. Representative maps are shown. A, aleurone; CA, crease aleurone; EMB, embryo; N, nucellar projection; P, pigment strand; PL, peripheral layers; SCU, scutellum. Scan size, 2000 × 2000 μm. Scale bars, 500 μm.

positive effects on the total element contents in the grain. Recently, nitrogen application has been demonstrated to enhance whole grain as well as endosperm Zn and Fe concentrations [28]. The mechanisms behind these increases have been attributed to nitrate-induced protein synthesis in the grain, which creates amplified Zn and Fe sinks in the endosperm [28]. Therefore, the form of Zn (Zn nitrate) used in this study might have additionally facilitated the increase in the grain Zn and Fe concentrations, although the grain size was not significantly affected. In addition, the changes observed in the micronutrient and macronutrient concentrations and in the Cd and Pb concentrations after Zn fertilization have presumably resulted from changes in the rhizosphere bioavailable fractions of these elements. These changes can significantly alter the amounts of the elements taken up by the plants, via competition of soil elements for the uptake, transport and storage, and/or interactions that take place within the plant itself [5]. However, in this small-sized experiment, with a small number of plants, the extreme Zn and nitrate concentrations used for soil fertilization do not

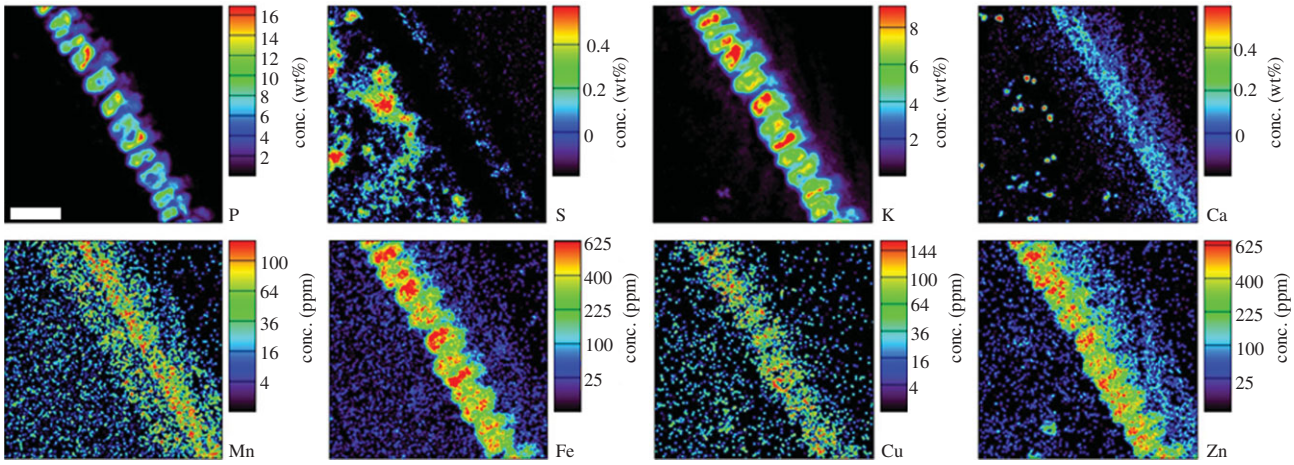

Figure 3. Micro-PIXE quantitative element maps from thin (60 μm) cross sections of wheat grain grown in Zn-fertilized soil. Scan location as in figure 1*c*. Scan size, 300 × 300 μm. Scale bar, 50 μm.

provide extensive conclusions as to the agronomical benefits of this Zn fertilization. Therefore, below, we focus in greater detail on the mineral element partitioning and its significance for the losses during grain milling.

The observed Zn-fertilization-induced decreases in P concentrations and contents indicate parallel reduced phytic acid concentrations [29], which lead to a desirable lower Zn to phytic acid ratio, and thus to enhanced availability of Zn during digestion. Additionally, Na and Mo concentrations and contents, as well as Mg, K, Mn, Cu and Cd contents, decreased after Zn fertilization. These effects might be the result of decreased P and associated phytic acid concentrations, i.e. fewer trapping sites for elements, assuming that the majority of these elements are physically complexed to phytate in globoids within protein storage vacuoles in the aleurone and in the scutellum [30–32]. Alternatively, they might reflect a higher efficiency of Zn–phytate complexation owing to the higher Zn concentration. Despite lower P concentrations found in a low phytic acid wheat genotype in comparison with wild-type [30], the concentrations or distribution of other elements within the grains [1,30] were not significantly altered. The observed Zn-fertilization-induced increases in Ca, Fe and Zn concentrations suggest that these elements are also bound to other molecular components in the grain. This was shown for Zn in barley grain embryo [33], was presumed for Fe in wheat grain endosperm and aleurone [34], and was determined for Ca on the basis of co-localization and on the highest abundance of Ca hotspots in endosperm, as revealed by micro-PIXE maps (this study).

It is generally assumed that tissue-specific and element-specific localization within the grain demonstrate that the transport and storage of the elements are under tight differential control, as has already been demonstrated using synchrotron X-ray fluorescence for Cd, Zn and Mn in rice nodes [35], and for Fe, Mn, Cu, K and Zn in mature barley grain [36]. Micro-PIXE has previously been used to determine the localization of P, S, Cl, K, Ca, Mn, Fe, Cu and Zn elements in wheat grain [10], but with limited spatial resolution (e.g. the average element contents were estimated without differentiation of the seed coat and the aleurone layer). In this study, micro-PIXE maps with improved resolution were acquired, which allowed the precise localization of specific elements in each of the individual tissues. The extraction of the element distribution profiles, which aid in the visualization of the concentration trends, has provided direct comparisons of the element concentrations in the grain from the non-fertilized and the Zn-fertilized plants. However, the interpretation of the quantitative spatial distributions of elements should always be performed with caution, especially when comparing bulk element concentrations, which provide an average across all of the tissues in the grain, and the element concentrations in particular sections, be they from grain or any other plant organ. Such comparisons often include discrepancies, which arise predominantly from three-dimensional variability in the tissue structure (i.e. the amount of a particular tissue contributing to the total mass of the organ or the grain) and this needs to be addressed individually. As the element distributions are usually highly heterogeneous, the presence of high proportions of tissues with low element concentrations (i.e. the endosperm in cereal grains) and low proportions of tissues with high element concentrations (i.e. the aleurone and the embryo in cereal grain) lead to dilution effects in the bulk analyses. In particular, wheat grain comprises 83 per cent as endosperm that is poor in minerals, 3 per cent as germ that is rich in minerals and 14 per cent of peripheral tissues (including the aleurone that is rich in minerals) [37]. Localization analyses are, on the other hand, performed for particular regions of the grain, and these give the average element concentrations in the particular sections themselves, which mainly depend on the amount of the particular tissue in the sections. In our case, we sectioned the grain at the embryo level. Thus, the concentrations of the majority of the elements obtained with micro-PIXE, the so-called section-specific concentrations (table 1), were generally slightly higher than those obtained with bulk analyses, with the exception of S, which is present at highest concentrations in the endosperm. Nevertheless, Zn-fertilization-related changes in bulk concentrations were seen in data obtained from micro-PIXE analysis of cross sections. Accordingly, while comparisons of absolute concentrations obtained from bulk analysis with those from (micro) imaging techniques are not straightforward, the main trends in changes are expected to be preserved.

The micro-PIXE element localization maps and distribution profiles obtained indicate that P and K were present mainly in the aleurone, scutellum and embryo. The localization of P to the aleurone is in line with the nanoscale

secondary ion mass spectrometry images of P localization in wheat grain [30] and with our data using synchrotron radiation X-ray fluorescence and microimaging [31], and this reflects the localization of phytate, i.e. the salts of phytic acid and mineral elements. The localization of K would thus correspond to phytate-bound K [32]. The strong co-localization of these two elements in the aleurone layer (but not in the peripheral layers, nor in the endosperm) is particularly evident in the micro-PIXE spatial distribution maps of thin sections. The majority of Fe and Zn appear to co-localize within the tissues of the wheat grain, with the nucellar projection especially rich in Fe. The mode of grain filling can be seen through the gradients of the concentrations from the vascular tissue and the aleurone layer to the endosperm, as has been demonstrated for Zn [3,38,39]. This gradient can be imaged in the grain without any chemical manipulation or extensive preparation procedures, which are avoided in micro-PIXE sample preparation. Additionally, micro-PIXE is, for now, the only technique that can routinely provide data in a quantitative manner [40]. The Zn concentration of the crease has been shown to be increased to very high levels by increasing the Zn supply, although the endosperm Zn concentrations did not increase correspondingly [39]. By contrast, our data demonstrate that the Zn endosperm concentrations also increased upon Zn fertilization of the soil. Nevertheless, the Zn transfer beyond the crease remains limited. In any case, uncovering the processes involved in this transfer, as well as understanding the contribution to the Zn distribution pathways from the crease to the central endosperm, require more research.

The nucellar projection can clearly be separated in the micro-PIXE maps from the Mn-rich and Ca-rich pigment strand. These two tissues are remnants of the grain nutritive tissue, from which the elements are distributed to their final locations during grain filling. As well as being predominantly located in the pigment strand, Mn and Ca were also localized to the peripheral layers, and especially to the intermediate layer. Within the endosperm (in the vicinity of the crease) and in the subaleurone layer, there are prominent Ca 'hot-spots' visible in the micro-PIXE distribution maps. These local increases in Ca concentrations would be masked in the relatively large volume of the endosperm of mechanically separated tissues and with concentrations determined chemically. Likewise, the uneven distribution of S in the endosperm, where the subaleurone endosperm cells are particularly rich in S, is of great interest. In comparison with other endosperm cells, subaleurone cells have been shown to be different in size and shape, and in size and abundance of starch granules, and to be especially rich in protein [41]. This is in agreement with an observed decrease in protein concentrations going from subaleurone cells to the central starchy endosperm cells [42]. It would be interesting to see whether there is any correlation between the unique spatial distribution of S and other micronutrients in the endosperm and of gluten protein in wheat endosperm. In thin-section mapping, there was almost no S in the aleurone layer, although there was some S in the intermediate layer, which is probably a remnant of the grain-filling processes. This point deserves further investigation.

In general, these observations further underline that the application of quantitative imaging techniques, such as the reported micro-PIXE analysis, to specific organ substructures is needed to advance our understanding of the complexity of element transport and storage in grain. This will consequently have important implications for the improvement of the nutritional content of cereal crops, and further on improving the element quality of milling fractions. This latter might be achieved by the development of advanced milling techniques with precise polishing, or of other methods for the gradual removal of the different tissues from the grain. In particular, the different distance of the Zn-rich part of the scutellum (mostly the innermost part of the scutellum) and that of the Fe-rich part (mainly the middle layer of the scutellum) from the peripheral tissue can be taken into account, as well as the strong partitioning of S, Cu and Mn in the intermediate layer of the pericarp. Thus, the separation of the milling fractions might be optimized to access high-Zn and/or high-Fe layers, or not to exclude the S-, Cu- and Mn-rich intermediate layer, to obtain their desired concentrations in the milling products.

Quantitative spatially resolved element profiles within wheat grain have revealed the precise location of the elements P, S, K, Ca, Mn, Fe, Cu and Zn at the tissue level. This knowledge is especially relevant as it can significantly contribute to the improvement of the quality of milling fractions, so as to provide desirable final element concentrations in the flours, and consequently in the flour products, in view of the need for the alleviation of micronutrient malnutrition. Furthermore, as no extensive manipulation of the samples (no chemical or mechanical disruption) is required for micro-PIXE analysis, the element profiles will help to explain the mode of grain filling for the various elements (including different grain developmental stages), which will foster advances in our understanding of the underlying processes involved in wheat grain element distributions during grain development. This knowledge can then be applied to the engineering of wheat cultivars with improved Fe and Zn qualities.

The work was supported by the following programmes and projects of the Slovenian Research Agency: P1-0212, P1-0112, J7-0352, J7-9805 and J4-2041, J1-4117, J4-4224, J4-3618, J7-0352, Z4-4113 and Fellowships for Young Researchers. Micro-PIXE instrumentation at JSI was partially upgraded within the seventh FP EU (project no. 227012 'SPIRIT'). The authors acknowledge Prof. Anton Tajnšek for providing the grain of the wheat cv. Reska used in this study. Dr Chris Berrie is acknowledged for English revision of the manuscript.

References

1. White PJ, Broadley MR. 2009 Biofortification of crops with seven mineral elements often lacking in human diets: iron, zinc, copper, calcium, magnesium, selenium and iodine. *New Phytol.* **182**, 49–84. (doi:10.1111/j.1469-8137.2008.02738.x)
2. McKevith B. 2004 Nutritional aspects of cereals. *BNF Nutr. Bull.* **29**, 111–142. (doi:10.1111/j.1467-3010.2004.00418.x)
3. Cakmak I, Pfeiffer WH, McClafferty B. 2010 Biofortification of durum wheat with zinc and iron. *Cereal Chem.* **87**, 10–20. (doi:10.1094/CCHEM-87-1-0010)
4. Ramesh SA, Choimes S, Schachtman DP. 2004 Over-expression of an *Arabidopsis* zinc transporter in *Hordeum vulgare* increases short-term zinc uptake

after zinc deprivation and seed zinc content. *Plant Mol. Biol.* **54**, 373–385. (doi:10.1023/B:PLAN.0000036370.70912.34)

5. Adams ML, Zhao FJ, McGrath SP, Nicholson FA, Chambers BJ. 2004 Predicting cadmium concentrations in wheat and barley grain using soil properties. *J. Environ. Qual.* **33**, 532–541. (doi:10.2134/jeq2004.0532)
6. Sarwar N, Saifullah, Malhi SS, Zia MH, Naeem A, Bibi S, Farid G. 2010 Role of mineral nutrition in minimizing cadmium accumulation by plants. *J. Sci. Food Agric.* **90**, 925–937. (doi:10.1002/jsfa.3916)
7. Grant CA, Bailey LD. 1997 Effects of phosphorus and zinc fertiliser management on cadmium accumulation in flaxseed. *J. Sci. Food Agric.* **73**, 307–314. (doi:10.1002/(SICI)1097-0010(199703)73:3<307::AID-JSFA732>3.0.CO;2-3)
8. Köleli N, Eker S, Cakmak I. 2004 Effect of zinc fertilization on cadmium toxicity in durum and bread wheat grown in zinc-deficient soil. *Environ. Pollut.* **131**, 453–459. (doi:10.1016/j.envpol.2004.02.012)
9. Cakmak I. 2008 Enrichment of cereal grains with zinc: agronomic or genetic biofortification? *Plant Soil* **302**, 1–17. (doi:10.1007/s11104-007-9466-3)
10. Mazzolini AP, Pallaghy CK, Legge GJF. 1985 Quantitative microanalysis of Mn, Zn and other elements in mature wheat seed. *New Phytol.* **100**, 483–509. (doi:10.1111/j.1469-8137.1985.tb02796.x)
11. Ozturk L *et al*. 2006 Concentration and localization of zinc during seed development and germination in wheat. *Physiol. Plant.* **128**, 144–152. (doi:10.1111/j.1399-3054.2006.00737.x)
12. Vogel-Mikuš K, Simčič J, Pelicon P, Budnar M, Kump P, Nečemer M, Mesjasz-Przybylowicz J, Przybylowicz WJ, Regvar M. 2008 Comparison of essential and non-essential element distribution in leaves of the Cd/Zn hyperaccumulator *Thlaspi praecox* as revealed by micro-PIXE. *Plant Cell Environ.* **31**, 1484–1496. (doi:10.1111/j.1365-3040.2008.01858.x)
13. Kachenko AG, Bhatia NP, Siegele R, Walsh KB, Singh B. 2009 Nickel, Zn and Cd localisation in seeds of metal hyperaccumulators using μ-PIXE spectroscopy. *Nucl. Instrum. Methods Phys. Res. B* **267**, 2176–2180. (doi:10.1016/j.nimb.2009.03.059)
14. Lombi E, Scheckel KG, Pallon J, Carey AM, Zhu YG, Meharg AA. 2009 Speciation and distribution of arsenic and localization of nutrients in rice grains. *New Phytol.* **184**, 193–201. (doi:10.1111/j.1469-8137.2009.02912.x)
15. Pongrac P, Vogel-Mikuš K, Regvar M, Vavpetič P, Pelicon P, Kreft I. 2011 Improved lateral discrimination in screening the element composition of buckwheat grain by micro-PIXE. *J. Agric. Food Chem.* **59**, 1275–1280. (doi:10.1021/jf103150d)
16. Udovic M, Lestan D. 2009 Pb, Zn and Cd mobility, availability and fractionation in aged soil remediated by EDTA leaching. *Chemosphere* **74**, 1367–1373. (doi:10.1016/j.chemosphere.2008.11.013)
17. Schneider T, Sheloske S, Povh B. 2002 A method for cryosectioning of plant roots for proton microprobe analysis. *Int. J. PIXE* **12**, 101–107. (doi:10.1142/S0129083502000196)
18. Pelicon P, Simčič J, Jakšič M, Medunić Z, Naab F, Mcdaniel FD. 2005 Spherical chamber—effective solution for multipurpose nuclear microprobe. *Nucl. Instrum. Methods Phys. Res. B* **231**, 53–59. (doi:10.1016/j.nimb.2005.01.034)
19. Simčič J, Pelicon P, Budnar M, Šmit Ž. 2002 The performance of the Ljubljana ion microprobe. *Nucl. Instrum. Methods Phys. Res. B* **190**, 283–286. (doi:10.1016/S0168-583X(01)01258-7)
20. Vogel-Mikuš K, Pelicon P, Vavpetič P, Kreft I, Regvar M. 2009 Element analysis of edible grains by micro-PIXE: common buckwheat case study. *Nucl. Instrum. Methods Phys. Res. B* **267**, 2884–2889. (doi:10.1016/j.nimb.2009.06.104)
21. Ryan CG. 2000 Quantitative trace element imaging using PIXE and the nuclear microprobe. *Int. J. Imaging Syst. Technol.* **11**, 219–230. (doi:10.1002/ima.1007)
22. Abramoff MD, Magalhães PJ, Ram SJ. 2004 Image processing with ImageJ. *Biophot. Int.* **11**, 36–42.
23. UL RS 68/96. 1996 Decree on input of dangerous substances and plant nutrients in the soil, Regulation Limits, Warning and Critical Values of Hazardous Substances in the Soil. *Official Gazette of the Republic of Slovenia* **68**, 5773–5774. [In Slovenian.]
24. Ribarič Lasnik C *et al*. 2002 Correlation studies of environmental pollution in the Upper Mežiška Valley in years from 1989 to 2001. Final report, ERICo, Velenje. [In Slovenian.]
25. Ristic Z, Bukovnik U, Prasad PVV, West M. 2008 A model for prediction of heat stability of photosynthetic membranes. *Crop Sci.* **48**, 1513–1522. (doi:10.2135/cropsci2007.11.0648)
26. Commission of the Euorpean Communities. 2006 Commission regulation EC 1881/2006 setting maximum levels for certain contaminants in foodstuffs. *Official J. Eur. Union* **49**, L364/5.
27. Zhao FJ, Su YH, Dunham SJ, Rakszegi M, Bedo Z, McGrath SP, Shewry PR. 2009 Variation in mineral micronutrient concentrations in grain of wheat lines of diverse origin. *J. Cereal Sci.* **49**, 290–295. (doi:10.1016/j.jcs.2008.11.007)
28. Kutman UB, Yildiz B, Cakmak I. 2011 Improved nitrogen status enhances zinc and iron concentrations both in the whole grain and the endosperm fraction of wheat. *J. Cereal Sci.* **53**, 118–125. (doi:10.1016/j.jcs.2010.10.006)
29. Erdal I, Yilmaz S, Taban S, Eker S, Torun B, Cakmak I. 2002 Phytic acid and phosphorus concentrations in seeds of wheat cultivars grown with and without zinc fertilisation. *J. Plant Nutr.* **25**, 113–127. (doi:10.1081/PLN-100108784)
30. Moore KL, Schröder M, Lombi E, Zhao FJ, McGrath SP, Hawkesford MJ, Shewry PR, Grovenor CRM. 2010 NanoSIMS analysis of arsenic and selenium in cereal grain. *New Phytol.* **185**, 434–445. (doi:10.1111/j.1469-8137.2009.03071.x)
31. Regvar M, Eichert D, Kaulich B, Gianonncelli A, Pongrac P, Vogel-Mikuš K, Kreft I. 2011 New insights into globoids of protein storage vacuoles in wheat aleurone using synchrotron soft X-ray microscopy. *J. Exp. Bot.* **62**, 3929–3939. (doi:10.1093/jxb/err090)
32. Joyce C, Deneau A, Peterson K, Ockenden I, Raboy V, Lott JNA. 2005 The concentrations and distributions of phytic acid phosphorus and other mineral nutrients in wild-type and low phytic acid Js-12-LPA wheat (*Triticum aestivum*) grain parts. *Can. J. Bot.* **83**, 1599–1607. (doi:10.1139/b05-128)
33. Persson DP, Hansen TH, Laursen KH, Schjoerring JK, Husted S. 2009 Simultaneous iron, zinc, sulfur and phosphorus speciation analysis of barley grain tissues using SEC-ICP-MS and IP-ICP-MS. *Metallomics* **1**, 418–426. (doi:10.1039/b905688b)
34. Moore KL, Zhao FJ, Gritsch CS, Tosi P, Hawkesford MJ, McGrath SP, Shewry PR, Grovenor CRM. 2012 Localisation of iron in wheat grains using high resolution secondary ion mass spectrometry. *J. Cereal Sci.* **55**, 183–187. (doi:10.1016/j.jcs.2011.11.005)
35. Yamaguchi N, Ishikawa S, Abe T, Baba K, Arao T, Terada Y. 2012 Role of the node in controlling traffic of cadmium, zinc, and manganese in rice. *J. Exp. Bot.* **63**, 2729–2737. (doi:10.1093/jxb/err455)
36. Lombi E *et al*. 2011 Megapixel imaging of (micro)nutrients in mature barley grains. *J. Exp. Bot.* **62**, 273–282. (doi:10.1093/jxb/erq270)
37. Barron C, Surget A, Rouau X. 2007 Relative amounts of tissues in mature wheat (*Triticum aestivum* L.) grain and their carbohydrate and phenolic acid composition. *J. Cereal Sci.* **45**, 88–96. (doi:10.1016/j.jcs.2006.07.004)
38. Wang YX, Specht A, Horst WJ. 2011 Stable isotope labelling and zinc distribution in grains studied by laser ablation ICP-MS in an ear culture system reveals zinc transport barriers during grain filling in wheat. *New Phytol.* **189**, 428–437. (doi:10.1111/j.1469-8137.2010.03489.x)
39. Stomph TJ, Choi EY, Stangoulis JCR. 2011 Temporal dynamics in wheat grain zinc distribution: is sink limitation the key? *Ann. Bot.* **107**, 927–937. (doi:10.1093/aob/mcr040)
40. McRae R, Bagchi P, Sumalekshmy S, Fahrni CJ. 2009 *In situ* imaging of metals in cells and tissues. *Chem. Rev.* **109**, 4780–4827. (doi:10.1021/cr900223a)
41. Kent NL. 1966 Subaleurone endosperm cells of high protein content. *Cereal Chem.* **43**, 585–601.
42. Tosi P, Parker M, Gritsch CS, Carzaniga R, Martin B, Shewry PR. 2009 Trafficking of storage proteins in developing grain of wheat. *J. Exp. Bot.* **60**, 979–991. (doi:10.1093/jxb/ern346)